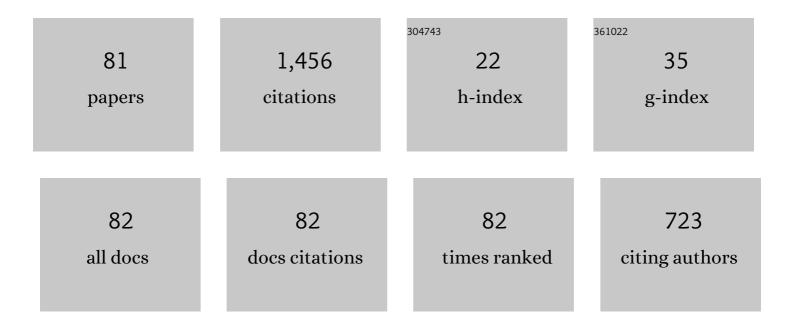
List of Publications by Year in descending order

Source: https://exaly.com/author-pdf/3551868/publications.pdf Version: 2024-02-01



#	Article	IF	CITATIONS
1	Direct observation of solidification behaviors of Fe-Mn-Si alloys during TIG spot welding using synchrotron X-ray. Scripta Materialia, 2022, 216, 114743.	5.2	6
2	Erratum to "Selection of the Massive-like <i>δ</i> - <i>γ</i> Transformation due to Nucleation of Metastable <i>δ</i> Phase in Fe-18 Mass%Cr-Ni Alloys with Ni Contents of 8, 11, 14 and 20 Mass%―[ISIJ International, Vol. 59 (2019), No. 3, pp. 459-465]. ISIJ International, 2021, 61, 1053-1053.	1.4	2
3	In situ observation of solidification crack propagation for type 310S and 316L stainless steels during TIG welding using synchrotron X-ray imaging. Journal of Materials Science, 2021, 56, 10653-10663.	3.7	12
4	Microstructural Evolutions of 2N Grade Pure Al and 4N Grade High-Purity Al during Friction Stir Welding. Materials, 2021, 14, 3606.	2.9	12
5	Influences of temperature and Sn-addition on microstructural evolution of Ag during FSW. Science and Technology of Welding and Joining, 2020, 25, 198-207.	3.1	4
6	Mechanism of grain structure development for pure Cu and Cu-30Zn with low stacking fault energy during FSW. Science and Technology of Welding and Joining, 2020, 25, 669-678.	3.1	14
7	Effect of Stacking Fault Energy on the Grain Structure Evolution of FCC Metals During Friction Stir Welding. Acta Metallurgica Sinica (English Letters), 2020, 33, 1001-1012.	2.9	30
8	Time-resolved X-ray imaging of solidification cracking for Al-Cu alloy at the weld crater. Materials Characterization, 2020, 167, 110469.	4.4	13
9	Time-resolved and <i>In-situ</i> Observation of <i>δ</i> – <i>γ</i> Transformation during Unidirectional Solidification in Fe–C Alloys. ISIJ International, 2020, 60, 930-938.	1.4	5
10	Friction Stir Welding of High Phosphorus Weathering Steel– Weldabilities, Microstructural Evolution and Mechanical Properties. Tetsu-To-Hagane/Journal of the Iron and Steel Institute of Japan, 2020, 106, 892-901.	0.4	5
11	Evaluation of dynamic development of grain structure during friction stir welding of pure copper using a quasi in situ method. Journal of Materials Science and Technology, 2019, 35, 1412-1421.	10.7	56
12	Role of annealing twinning in microstructural evolution of high purity silver during friction stir welding. Science and Technology of Welding and Joining, 2019, 24, 644-651.	3.1	7
13	Strain rate dependent micro-texture evolution in friction stir welding of copper. Materialia, 2019, 6, 100302.	2.7	23
14	Time-resolved and <i>In-situ</i> Observation of δ-γ Transformation during Unidirectional Solidification in Fe-C Alloys. Tetsu-To-Hagane/Journal of the Iron and Steel Institute of Japan, 2019, 105, 290-298.	0.4	14
15	Selection of the Massive-like <i>Î'</i> - <i>γ</i> Transformation due to Nucleation of Metastable <i>Î'</i> Phase in Fe-18 Mass%Cr-Ni Alloys with Ni Contents of 8, 11, 14 and 20 Mass%. ISIJ International, 2019, 59, 459-465.	1.4	13
16	Experimental evaluation of strain and strain rate during rapid cooling friction stir welding of pure copper. Science and Technology of Welding and Joining, 2019, 24, 352-359.	3.1	47
17	Semi-solid deformation of Al-Cu alloys: A quantitative comparison between real-time imaging and coupled LBM-DEM simulations. Acta Materialia, 2019, 163, 208-225.	7.9	23
18	In situ Observation Using Synchrotron Radiation. Yosetsu Gakkai Shi/Journal of the Japan Welding Society, 2019, 88, 274-278.	0.1	0

#	Article	IF	CITATIONS
19	Microstructure evolution of Cu–30Zn during friction stir welding. Journal of Materials Science, 2018, 53, 10423-10441.	3.7	31
20	Investigation of temperature dependent microstructure evolution of pure iron during friction stir welding using liquid CO2 rapid cooling. Materials Characterization, 2018, 137, 24-38.	4.4	33
21	X-Ray Imaging of Formation and Growth of Spheroidal Graphite in Ductile Cast Iron. Materials Science Forum, 2018, 925, 104-109.	0.3	5
22	Dilatancy in semi-solid steels at high solid fraction. Acta Materialia, 2017, 125, 187-195.	7.9	40
23	<i>In-situ</i> Measurement of Solute Partition Coefficient in Fe-Cr-Ni-Mo Alloys by Using X-ray Imaging and X-ray Florescence Analysis. Tetsu-To-Hagane/Journal of the Iron and Steel Institute of Japan, 2017, 103, 678-687.	0.4	6
24	<i>In Situ</i> Observations of Tensile and Compressive Deformations in Semi Solid Metallic Alloys Using Time-resolved X-ray Imaging. Tetsu-To-Hagane/Journal of the Iron and Steel Institute of Japan, 2017, 103, 668-677.	0.4	5
25	<i>In situ</i> Observation of Dendrite Growth in Sn-Bi Alloys under Ultrasonic Vibration Using Time-resolved X-ray Imaging. Tetsu-To-Hagane/Journal of the Iron and Steel Institute of Japan, 2016, 102, 170-178.	0.4	3
26	Impacts of Interface Energies and Transformation Strain from BCC to FCC on Massive-like δ-γ Transformation in Steel. IOP Conference Series: Materials Science and Engineering, 2015, 84, 012049.	0.6	10
27	Interface Energies of Hetero- and Homo-Phase Boundaries and Their Impact on δ-γ Massive-Like Phase Transformations in Carbon Steel. Materials Transactions, 2015, 56, 1461-1466.	1.2	18
28	Concurrent γ-Phase Nucleation as a Possible Mechanism of δ-γ Massive-like Phase Transformation in Carbon Steel: Numerical Analysis Based on Effective Interface Energy. Materials Transactions, 2015, 56, 1467-1474.	1.2	17
29	Yet Another Marked Difference among Impurities as Modifier Elements for Refinement of Eutectic Si in Al-Si Alloys. Materials Transactions, 2015, 56, 1475-1483.	1.2	5
30	Application of a macroscopic model to predict the band segregation induced by shear deformation of semisolid. IOP Conference Series: Materials Science and Engineering, 2015, 84, 012011.	0.6	0
31	Impact of melt convection induced by ultrasonic wave on dendrite growth in Sn–Bi alloys. Materials Letters, 2015, 150, 135-138.	2.6	30
32	Influence of Mg on Solidification of Hypereutectic Cast Iron: X-ray Radiography Study. Metallurgical and Materials Transactions A: Physical Metallurgy and Materials Science, 2015, 46, 4937-4946.	2.2	28
33	Localization of shear strain and shear band formation induced by deformation in semi-solid Al-Cu alloys. IOP Conference Series: Materials Science and Engineering, 2015, 84, 012078.	0.6	1
34	Kinetics of the δ/γ interface in the massive-like transformation in Fe-0.3C-0.6Mn-0.3Si alloys. IOP Conference Series: Materials Science and Engineering, 2015, 84, 012062.	0.6	19
35	Flowering of Continuous Casting Process for Steel in Japan and New Fundamental Seeds to the Future. Tetsu-To-Hagane/Journal of the Iron and Steel Institute of Japan, 2014, 100, 472-484.	0.4	10
36	In Situ Observation of Deformation in Semi-solid Fe-C Alloys at High Shear Rate. Metallurgical and Materials Transactions A: Physical Metallurgy and Materials Science, 2014, 45, 5613-5623.	2.2	17

#	Article	IF	CITATIONS
37	Synchrotron Radiography Studies of Shear-Induced Dilation in Semisolid Al Alloys and Steels. Jom, 2014, 66, 1415-1424.	1.9	13
38	In Situ Observation of Solidification Behaviors in Carbon Steels Using Synchrotron X-ray Imaging. Materia Japan, 2014, 53, 467-470.	0.1	0
39	Development in In Situ Observation of Deformation in Semi-solid Alloys Using X-Ray Imaging. , 2014, , 231-243.		2
40	Real time synchrotron X-ray observations of solidification in hypoeutectic Al–Si alloys. Materials Characterization, 2013, 85, 134-140.	4.4	34
41	Advanced Analysis of Solidification by X-ray Imaging. , 2013, , 93-104.		0
42	In situ study of granular micromechanics in semi-solid carbon steels. Acta Materialia, 2013, 61, 4169-4179.	7.9	34
43	Characterization of Shear Deformation Based on In-situ Observation of Deformation in Semi-solid Al–Cu Alloys and Water-particle Mixture. ISIJ International, 2013, 53, 1195-1201.	1.4	21
44	Characterization of Shear Deformation Based on In-situ Observation of Deformation in Semi-Solid Al-Cu Alloys and Water-Particle Mixture. Tetsu-To-Hagane/Journal of the Iron and Steel Institute of Japan, 2013, 99, 141-148.	0.4	2
45	In-situobservation of peritectic solidification in Sn-Cd and Fe-C alloys. IOP Conference Series: Materials Science and Engineering, 2012, 27, 012084.	0.6	25
46	Macroscopic modelling of semisolid deformation for considering segregation bands induced by shear deformation. IOP Conference Series: Materials Science and Engineering, 2012, 33, 012053.	0.6	5
47	Direct Observation of Shear Deformation in Semi-solid Alloys Using X-ray Imaging. Materia Japan, 2012, 51, 561-568.	0.1	1
48	Fabrication of Al <sub>2</sub> O <sub>3</sub> –YAG Equilibrium Eutectic Composites via Transformation from Fine Al <sub>2</sub> O <sub>3</sub> and YAP Powder Mixtures. Materials Transactions, 2012, 53, 1124-1129.	1.2	4
49	Massive transformation from <i>δ</i> phase to <i>γ</i> phase in Fe–C alloys and strain induced in solidifying shell. IOP Conference Series: Materials Science and Engineering, 2012, 33, 012036.	0.6	38
50	Synchrotron radiography of direct-shear in semi-solid alloys. IOP Conference Series: Materials Science and Engineering, 2012, 27, 012086.	0.6	9
51	Solidification of Al2O3–YAG eutectic composites with off-metastable eutectic composition from undercooled melt produced by melting Al2O3–YAP eutectics. Journal of the European Ceramic Society, 2012, 32, 2137-2143.	5.7	7
52	Development of X-ray Imaging for Observing Solidification of Carbon Steels. ISIJ International, 2011, 51, 402-408.	1.4	100
53	放射å‰ã,'å^©ç"¨ã⊷ãŸã,¢ãƒ«ãƒŸãƒ«ã,¦ãƒå•́é‡ʿã®å‡å>°ç¾è±jã®è§£æ~Ž. Keikinzoku/Journal of Japan Instit	ute@faLigh	nt Mætals, 20

54 Direct observation of deformation in semi-solid carbon steel. Scripta Materialia, 2011, 64, 1129-1132.

5.2 81

#	Article	IF	CITATIONS
55	Granular deformation mechanisms in semi-solid alloys. Acta Materialia, 2011, 59, 4933-4943.	7.9	89
56	In situ investigation of unidirectional solidification in Sn–0.7Cu and Sn–0.7Cu–0.06Ni. Acta Materialia, 2011, 59, 4043-4054.	7.9	56
57	Microstructural Control and Development of Synthesis Route for Enhancing Performance of Sintered Thermoelectric Oxide Polycrystals via Chemical Solution Process. Funtai Oyobi Fummatsu Yakin/Journal of the Japan Society of Powder and Powder Metallurgy, 2010, 57, 224-231.	0.2	3
58	Regular Structure Formation of Hypermonotectic Al-In Alloys. Materials Science Forum, 2010, 649, 131-136.	0.3	4
59	Three-dimensional alignment of FeSi <sub>2</sub> with orthorhombic symmetry by an anisotropic magnetic field. Journal of Physics: Conference Series, 2009, 165, 012021.	0.4	13
60	Chain structure in the unidirectionally solidified Al2O3–YAG–ZrO2 eutectic composite. Journal of Crystal Growth, 2009, 311, 3765-3770.	1.5	13
61	<i>In situ</i> observation of solidification phenomena in Al–Cu and Fe–Si–Al alloys. International Journal of Cast Metals Research, 2009, 22, 15-21.	1.0	81
62	Formation and microstructure of Al <sub>2</sub> O <sub>3</sub> -YAG eutectic ceramics by phase transformation from metastable system to equilibrium system. Journal of Physics: Conference Series, 2009, 165, 012006.	0.4	5
63	Crystal growth in the bulk-metallic-glass Zr-based alloys by using the DC + AC levitation method. Journal of Physics: Conference Series, 2009, 144, 012056.	0.4	1
64	<i>In situ</i> observation of nucleation, fragmentation and microstructure evolution in Sn–Bi and Al–Cu alloys. International Journal of Cast Metals Research, 2008, 21, 125-128.	1.0	48
65	Effects of Shaping Conditions on the Microstructure and the Mechanical Property of the Al <sub>2</sub> O <sub>3</sub> -YAG Eutectic Composite Produced by Melting the Al <sub>2</sub> O <sub>3</sub> -YAP Eutectic Structure. Materials Transactions, 2007, 48, 2312-2315.	1.2	5
66	Effect of the Melt Flow on the Solidified Structure of Middle Carbon Steel by Means of the Levitation Method Using Alternating and Static Magnetic Fields. ISIJ International, 2007, 47, 612-618.	1.4	14
67	Three-dimensional Observation of Al <sub>2</sub> O <sub>3</sub> -GAP Eutectic Structure by X-ray Micro CT. Materia Japan, 2007, 46, 819-819.	0.1	1
68	Thermoelectric properties of NaxCo2O4 with rare-earth metals doping prepared by polymerized complex method. Journal of Alloys and Compounds, 2006, 408-412, 1217-1221.	5.5	19
69	Nucleation and Growth in Undercooled Melts of Bulk-Metallic-Glass Forming Zr <sub>60</sub> Ni <sub>25</sub> Al <sub>15</sub> Alloy. Materials Transactions, 2005, 46, 2762-2767.	1.2	14
70	Effect of the Polymerized Complex Process on Doping Limit of Thermoelectric Na <l><sub>x</sub></l> Co <sub>1−<l>y</l></sub> M <l><sub>y</sub></l> O <sub>2</sub> (M=Mn,)	Tj £₽Qq0	0 @ <b>3</b> gBT /Ove
71	SYNTHESIS OF NaxCo2O4 THERMOELECTRIC OXIDE BY THE POLYMERIZED COMPLEX METHOD AND SPS METHODS. , 2005, , 317-320.		0

<sup>&</sup>lt;sup>72</sup> Synthesis of NaxCo2O4thermoelectric oxide with crystallographic anisotropy by chemical solution process. Science and Technology of Advanced Materials, 2004, 5, 125-131.

#	Article	IF	CITATIONS
73	Effect of Partial Substitutions of Rare-earth Metals for Na-site on the Thermoelectric Properties of Na <sub><i>x</i></sub> Co <sub>2</sub> O <sub>4</sub> Prepared by the Polymerized Complex Method. Materials Transactions, 2004, 45, 1339-1345.	1.2	11
74	Thermoelectric Properties of (Na1-yMy)xCo2O4 (M: K, Sr, Y, Nd, Sm and Yb; y = 0.01â‰^0.35) ChemInform, 2003, 34, no.	0.0	1
75	Thermoelectric properties of (Na1â^'yMy)xCo2O4 (M=K, Sr, Y, Nd, Sm and Yb; y=0.01â^¼0.35). Journal of Alloys and Compounds, 2003, 348, 263-269.	5.5	52
76	Thermoelectric Properties of Na <sub>x</sub> Co <sub>2</sub> O <sub>4</sub> Prepared by the Polymerized Complex Method and Hot-Pressing. Materials Transactions, 2003, 44, 155-160.	1.2	6
77	Thermoelectric Properties of Na <sub>x</sub> Co <sub>2</sub> O <sub>4</sub> Prepared by the Polymerized Complex Method and Spark Plasma Sintering. Materials Transactions, 2003, 44, 1866-1871.	1.2	11
78	Effect of Partial Substitution of 3d Transition Metals for Co on the Thermoelectric Properties of Na <sub>x</sub> Co <sub>2</sub> O <sub>4</sub> . Materials Transactions, 2002, 43, 601-604.	1.2	25
79	Microstructure and Thermoelectric Properties of NaxCo2O4 Synthesized by Spark Plasma Sintering Funtai Oyobi Fummatsu Yakin/Journal of the Japan Society of Powder and Powder Metallurgy, 2002, 49, 406-411.	0.2	8
80	Thermoelectric properties of Na/sub x/Co/sub 2/O/sub 4/ prepared by the polymerized complex method. , 0, , .		0
81	<i>In Situ</i> Study of the Altering Globule Packing-Density during Semisolid Alloy Deformation. Solid State Phenomena, 0, 192-193, 185-190.	0.3	0